Effect of added resonators in RFID system at 13.56 MHz

Megdouda Benamara, Marjorie Grzeskowiak, Antoine Diet, Christophe Conessa, Gaelle Bazin Lissorgues, Yann Le Bihan

Effect of added resonators in RFID system at 13.56 MHz

Megdouda Benamara[1] ✉, Marjorie Grzeskowiak[1], Antoine Diet[2], Christophe Conessa[2], Gaëlle Lissorgues[1], Yann Le Bihan[2]

[1]*ESYCOM (EA 2552), UPEMLV, ESIEE-Paris, CNAM, 77454 Marne-la-Vallée, France*

[2]*GeePs (UMR 8507), CNRS, CentraleSupelec, Paris-Sud University, UPMC, 91192 Gif-sur-Yvette, France*

✉ *E-mail: benamara@univ-mlv.fr*

Abstract: In this study, a reader antenna including resonators is proposed to improve detection of a small moving tag in the case of tracking a radiofrequency identification (RFID) system. The near-field RFID technology is based on load modulation, the input impedance on the reader coil and the mutual inductance between the reader and tag coils are the main parameters for performing detection. They are calculated from the impedance matrix parameters. The added resonators change all the parameters of the impedance matrix consequently the input impedance and mutual inductance are also changed. In this study, analytical formulation defining the equivalent impedance matrix parameters is developed. These formulae are used to evaluate the performance of the proposed design according to the tag misalignment (lateral and angular). From the calculation and simulation results, a frequency shift in the equivalent input impedance is found. To avoid this problem, optimising the positioning of the resonators on the reader coil is performed. This study is confirmed by measures of RFID detection for a reader prototype (with and without resonators) and a small commercial tag. Both the surface and volume of detection of the small moving tag (lateral and angular misalignment) are improved by the principle of added resonators.

1 Introduction

Nowadays the use of wireless communication systems is constantly increasing. Wireless systems are required for different applications such as wireless charging, tracking, medical diagnostic and radiofrequency identification (RFID) thanks to inductive coupling with the constraint of a short range distance but also for systems working in dissipative or disrupting media, such as sea water, metallic environment and biological tissues [1–6]. Each of these applications, as its need arises, has to respect some specifications like: the frequency [low frequency, high frequency (HF) etc.], the distance of communication, the size and shape of the transmitter and receiver coils despite their lateral and angular positioning [7–13]. As is known, the HF RFID system is composed of two parts: the reader and the tag. The reader is an electronic circuit linked to a coil antenna. The tag is a combination of the coil antenna and a chip. Communication between the two parts is done by the principle of load modulation: the reader antenna generates a magnetic field; this is served to create communication with the tag by magnetic coupling. The distribution of the magnetic field generated by the reader coil depends on its physical and electrical properties. Following the principle of load modulation, a variation of the chip impedance is seen in the tag part; this variation is interpreted by detection in the reader circuit. In brief, RFID detection can be reduced to two specific parameters: the input impedance of the reader and the mutual inductance between the reader and tag coils. These parameters are depending on both the electrical and physical properties of the reader and tag coils. One of the most known constraints in practice is the limited size of the tag (the size of the tag depends on the size of the object to identify); also detection is depending on the displacement of the tag (lateral and angular displacement). Hence, to optimise detection, two-fold objectives must be satisfied; diversity of B-field orientation and uniform B-field magnitude distribution to propose efficient inductive link versus the orientation and position of the small tag above the reader coil. To improve the detection range whatever the lateral and angular misalignments of the received coil, the generated magnetic field can be maximised by maintaining constant feed power: it is an essential need. In the literature, many studies have proposed in this way by modifying the geometrical coil of the transmitter [14–17].

HF RFID applications are distinct to tracking animals or objects, feeding objects with required low power like biomedical sensors or identification for security control. In the case of tracking tag application, the greater difficulty is the requirement of minimum energy to be provided to the tag whatever its positioning above the reader coil. As is said in [11–19], the generated magnetic field by a conventional reader coil decreases at its surface, and has a specific orientation of the magnetic field lines. The distance of detection and the misalignment of the tag (lateral and angular) are then strongly limited by the principle of magnetic field distribution. To avoid this difficulty (ensure the continuity of detection despite the size ratio between the reader and tag coils, the lateral misalignment of the tag coil and the different angular orientations of the tag coil), a solution to the coplanar added resonator on the surface of the reader coil is proposed in [20]. The added resonator has two main advantages: change the distribution of the magnetic field and reduce the size ratio between the reader and tag coils. This principle can create new zones of detection required by the moving tag in different angular orientations. The proposed design of the RFID system is confirmed by improvement of the magnetic coupling parameters of the system (mutual inductance, input impedance, and RFID detection). In contrast, as is proved by calculation in [20], the electrical parameters of the system (impedance matrix parameters) are modified by the added resonator, this can positively (improving RFID detection) and negatively (frequency shift) affect the performance of the RFID system. Only the positive effects of the proposed system are developed in [20] to confirm its interest.

In this study, the positive and negative effects of the proposed solution of added resonators on the reader coil are studied. The principle of added resonators is, firstly, developed for a prototype of a reader coil including one resonator. In the following section, the impedance matrix of the RFID system including one resonator is calculated and compared with the system without the resonator. The prototype of a reader antenna including one resonator is studied versus the lateral misalignment of the tag above the surface

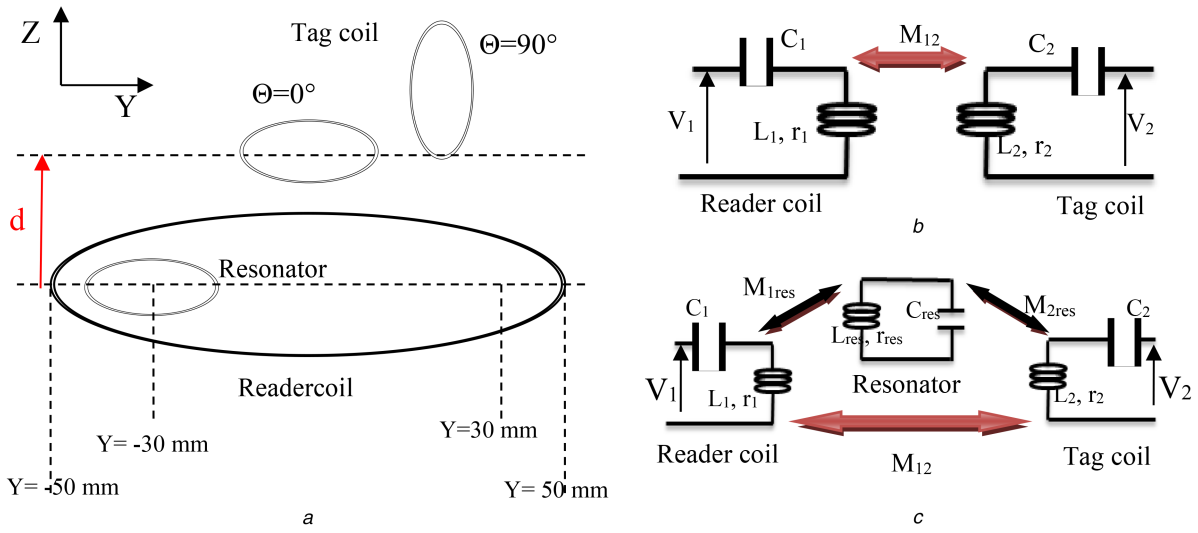

Fig. 1 *Proposed reader coil including*
(a) One resonator, **(*b*)** Its electrical model without resonator, ***(c)*** Its electrical model with resonator

of the reader coil and for two angular orientations of the tag coil: parallel configuration ($\theta = 0°$) and perpendicular configuration ($\theta = 90°$). To confirm the interest of the proposed solution, mutual inductance and input impedance are fixed as our figures of merit and used to compare the proposed design to the conventional RFID system (without a resonator). The analytical formulae defining the equivalent electrical model of the system are used in simulation part. From calculation and simulation results, the added resonator improves both the mutual inductance and the magnitude of input impedance. In contrast, the added resonator affects all the impedance matrix parameters: if the phase of the equivalent input impedance of the reader coil is changed, null detection could appear because of the frequency shift. The shift frequency is studied by simulation, using the analytical calculation of the equivalent input impedance of the system in the third section of this paper. In the last section, a prototype of a reader coil including two resonators is studied. The analytical calculation of equivalent impedance parameters is developed; in this case, the impedance matrix is changed by the properties of the added resonators and also by the magnetic coupling between the two resonators. To confirm experimentally the study, a large prototype of the reader antenna including two resonators is fabricated to evaluate the frequency shift of the reader input impedance according to the number of added resonators (zero, one and two resonators). Finally, the proposed prototype is validated by detection measurements using a small circular commercial tag.

2 Analytical study

Firstly a system of reader coil including one resonator is studied. According to the equivalent electrical model in Fig. 1*b* and as developed in [17], the impedance matrix is changed in the equivalent impedance matrix. The parameters, in this case, are expressed by the following equation:

$$\begin{aligned}
Z_{11_{eq}} &= j\omega\left(L_1 - \frac{1}{C_1\omega^2} + \omega(M_{1res})^2\gamma\right) + \omega^2(M_{1res})^2\delta + r_1,\\
Z_{12_{eq}} &= j\omega(M_{12} + \omega M_{1res}M_{2res}\gamma) + \omega^2 M_{1res}M_{2res}\delta,\\
Z_{21_{eq}} &= j\omega(M_{21} + \omega M_{2res}M_{1res}\gamma) + \omega^2 M_{2res}M_{1res}\delta,\\
Z_{22_{eq}} &= j\omega\left(L_2 - \frac{1}{C_2\omega^2} + \omega(M_{2res})^2\gamma\right) + \omega^2(M_{2res})^2\delta + r_2.
\end{aligned} \tag{1}$$

With

$$\gamma = \frac{(1/C_{res}\omega) - \omega L_{res}}{(\omega L_{res} - (1/C_{res}\omega))^2 + r_{res}},$$

$$\delta = \frac{r_{res}}{((1/C_{res}\omega) - \omega L_{res})^2 + r_{res}}.$$

Whoever is in the case of the conventional system, the impedance matrix parameters are expressed by the following equation:

$$\begin{aligned}
Z_{11_{eq}} &= j\omega\left(L_1 - \frac{1}{C_1\omega^2}\right) + r_1,\\
Z_{12_{eq}} &= j\omega(M_{12}),\\
Z_{21_{eq}} &= j\omega(M_{12}),\\
Z_{22_{eq}} &= j\omega\left(L_2 - (1/C_2\omega^2)\right) + r_2.
\end{aligned} \tag{2}$$

From (1) and (2), we can deduce the effect of the added resonators on all the impedance matrix parameters. The influence is depicted by the mutual inductance between the resonators and reader coil, the mutual inductance between the tag and resonator and also on the electrical properties of the resonator.

3 Simulation results

3.1 Magnetic field

To validate the principle of reader coil including resonators, the proposed prototype in Fig. 1 is studied by HF electromagnetic field simulation. The design is composed of three coils: the reader, the resonator, and the tag. Their electrical properties are summarised in Table 1.

The coils of the reader, the resonators, and the tag have, respectively, radii of 50, 15 and 15 mm. The capacitances are added to realise a resonant circuit at 13.56 MHz frequency.

Adding coplanar resonators inside the reader surface can be understood by B-field display. In Fig. 2, the generated magnetic field in the (*X*, *Y*) and (*Y*, *Z*) planes from the conventional reader coil are compared with the one provided by the reader coil including one resonator.

As seen on Fig. 2*a* and *b*, the generated magnetic field in the case of a conventional reader coil has a maximum around the edges of the reader coil. The distribution of the magnetic field decreases in the direction of the centre of the coil. The added resonator changes this distribution. A maximum of the magnitude of the magnetic field can be seen around the edges of the resonator. Between the edges of the resonator and the centre of the reader coil, a zero generated magnetic field is seen. This is due to the sum of the generated magnetic field because of the sense and direction of the current in the reader and the resonator coils.

Table 1 Electrical properties of the proposed prototype

	Inductance	Resistance	Capacitance
reader	$L_1 = 0.3$ μH	$r_1 = 0.1$ Ω	$C_1 = 0.45$ nF
resonator	$L_{res} = 0.058$ μH	$r_2 = 0.06$ Ω	$C_2 = 2.32$ nF
tag	$L_2 = 0.058$ μH	$r_2 = 0.06$ Ω	$C_2 = 2.32$ nF

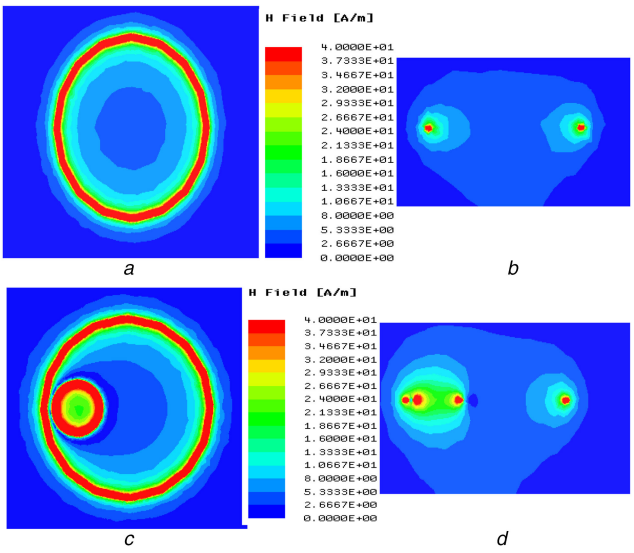

Fig. 2 *Generated magnetic field according to the (X, Y) and the (Y, Z) plans.*
(a,b) by the conventional reader coil and ***(c,d)*** by the reader coil including resonator.

3.2 Effect of the resonator positioning

In this section, the different mutual inductances M_{1res} (between the resonator and reader coil) and M_{2res} (between the resonator and tag coil) in (1) are studied to optimise the resonator positioning on the reader surface. The tag coil is positioned firstly at the centre of the reader coil at 10 mm away from the reader surface. Then the resonator is moving above the surface; its positioning is varied from $Y = -30$ mm to $Y = 30$ mm as shown in Fig. 1*a*. Results are presented for parallel and perpendicular configurations. In Fig. 3*a*, the mutual inductance between the resonator and reader coil is reported in the presence of the tag. For both configurations, the same behaviour and values are observed for the mutual inductance according to the resonator positioning: the maximum value appears for the resonator near the edges of the reader coil, while the value decreases up to a minimum for the resonator moving away from the edge to the centre of the reader coil. This variation is in accordance with the B-field display (Fig. 2*a*), where the maxima are seen around the edges of the coil and minima at its centre. For both parallel and perpendicular configurations of the tag, the generated magnetic field is not affected; hence the mutual inductance between the reader coil and resonator does not depend upon the tag.

Figs. 3*b* and *c* present, respectively, the mutual inductance between the tag and moving resonator for parallel and perpendicular configurations of the tag with the tag position kept constant, i.e. in the centre of the coil. For the parallel configuration (Fig. 3*b*), the maximum of the mutual inductance is seen at $Y_{res} = 0$ mm when the resonator is positioned at the centre of the reader coil. The mutual inductance is decreased when the positioning of the resonator is varied from the centre of the reader coil to its edges (from −30 to 0 mm or from 30 to 0 mm): the tag receives the maximum of the magnetic field for the coaxial position with the resonator. In the perpendicular configuration for a tag in the coil centre, the mutual inductance has two maxima corresponding to $Y_{res} = -15$ mm and $Y_{res} = 15$ has and zero value at the centre coil ($Y_{res} = 0$ mm) because of the distribution of the magnetic field (Fig. 2). The maximum value for mutual inductance in a parallel configuration (Fig. 3*b*) is higher up to 5 times in comparison with the one in the perpendicular configuration (Fig. 3*c*). The best positioning of the resonator in terms of maximum mutual inductance with the reader is clearly seen near to its edges. For the following study, the resonator is positioned at $y = -30$ mm as shown in Fig. 1*a*. In dedicated applications, the tag will be moving and rotating above the reader surface and the resonator positioning allows favouring inductive coupling in specific areas.

3.3 Effect of the added resonators on the equivalent mutual inductance

From (1), the equivalent mutual inductance is calculated by using the following equation:

$$M_{eq} = M_{12} + \omega M_{1res} M_{res2} \gamma . \quad (3)$$

The equivalent mutual inductance in (3) is used to evaluate the performance of the proposed design for the misaligned tag (lateral and angular misalignment). In Fig. 4, the equivalent mutual inductance between the misaligned tag (from $y = -100$ mm to $y = 100$ mm) in parallel and perpendicular configurations is reported. The resonator is positioned at $y = -30$ mm (near to the edges of the reader coil) according to the results of the last section (Fig. 4). The distance between the reader coil including the resonator and the tag is fixed at 10 mm. In the parallel configuration (Fig. 4*a*), the maximum of equivalent mutual inductance (22 nH) is seen above the surface corresponding to the centre of the resonator (as confirmed by the results in Figs. 3*a* and *b*). Near the edges of the reader coil, the second maximum of 11 nH can be seen corresponding to the zone where maximum B-field can be seen in Fig. 2: the added resonator improves above its surface the equivalent mutual inductance by 11 nH (from 11 to 22 nH). The minimum of equivalent mutual inductance is seen in the centre of the reader coil as expected from the B-field distribution in Figs. 2*c* and *d*. In the perpendicular configuration (Fig. 4*a*), the added resonator creates a shift of the zero for the equivalent mutual inductance: in the conventional RFID system, the zero mutual inductance for the perpendicular configuration is seen at the centre of the reader coil. Also, the maximum of mutual inductance is improved by 2 nH above the surface of the resonator compared with the case without a resonator (the improvement of the mutual inductance is calculated by comparing the value of the equivalent mutual inductance between (-100 mm $< y < 0$ mm) corresponding to the area of the reader coil including the resonator and (0 mm $< y < 100$ mm) which is the part of the reader coil which does not include the resonator. As shown in Fig. 4, the equivalent mutual inductance has better values in the parallel configuration. According to the mutual inductance and depending on the area, the maximum RFID read-out distance could be greater for the parallel configuration by comparison with the r tag placed perpendicular to the reader surface. In the following section, the impact of the inductive coupling on the tag can be seen in the reader input impedance.

3.4 Effect of the added on the equivalent input impedance

The effect of the added resonator on the input impedance (magnitude and phase) of the reader coil is studied.

The positioning of the resonator strengthens the inductive coupling between the resonator and the reader coil, as seen previously in Fig. 3*a*. An analytical formula of the equivalent input impedance is given. In the calculated equivalent impedance parameters (1), previous parameters appear the mutual inductance between the reader coil and the resonator (M_{1res}), the mutual inductance between the tag coil and the resonator (M_{2res}) and the two factors (γ, δ) related to the electrical properties of the

resonator. In the conventional RFID system (Fig. 5*a*), the input impedance is calculated from the impedance matrix parameters and the impedance of the tag chip. To perform detection, the magnitude of the input impedance would be efficient whatever the positioning of the tag (distance, lateral and angular positioning). Its phase must be invariable to ensure detection. In this case, the input impedance is calculated by using the following equation:

$$Z_{\text{in}} = Z_{11} - \frac{Z_{12}^2}{Z_{22} + Z_{\text{chip}}} = \text{jIm}(Z_{\text{in}}) + \text{Re}(Z_{\text{in}}). \quad (4)$$

According to the calculated equivalent impedance parameters, the equivalent input impedance in the case of the reader antenna including one resonator (Fig. 5*b*) can be calculated by using the following equation:

$$Z_{\text{in}_{\text{eq}}} = Z_{11_{\text{eq}}} - \frac{Z_{12_{\text{eq}}}^2}{Z_{22_{\text{eq}}} + Z_{\text{chip}}} = \text{jIm}(Z_{\text{in}_{\text{eq}}}) + \text{Re}(Z_{\text{in}_{\text{eq}}}). \quad (5)$$

As we can see in (5), all the parameters of the calculation of equivalent input impedance are changed compared with (4).

To evaluate the influence of the resonator on the input impedance, (4) and (5) are used. In Fig. 6, the magnitude and phase of the input and equivalent input impedances are reported in both parallel and perpendicular configurations. The simulated results are presented for the misaligned tag (100 mm < Y < 100 mm) at a distance of 10 mm.

For the parallel configuration, in the case of a conventional system, the magnitude of the equivalent input impedance has two maxima up to 5 Ω above the edges of the reader coil. At the surface of the reader coil we can see a variation of the magnitude of the input impedance but this variation is very low (From 5 to 2 Ω). However, the added resonator changes the variation of the magnitude of the equivalent input impedance. In this case, the magnitude of the equivalent input impedance presents three maxima; two maxima corresponding to the edges of the reader coil (6.5 Ω) and a peak of 12 Ω above the surface of the reader coil including the resonator. The variation of the magnitude of the input impedance (from 6.5 to 12 Ω) is higher compared with the case of a system without the resonator. Also, the variation of the phase of the equivalent input impedance is seen above the surface of the reader antenna including the resonator (between 50 and −10 mm). In the case of the conventional system, the phase of the input impedance is kept constant above the surface of the reader coil (80°).

In the perpendicular configuration, the magnitude of the equivalent input impedance has a maximum value of 4.5 Ω corresponding to the surface of the reader including the resonator (maximum value at the edges of the reader $y = -50$ mm because of the best condition of coupling between the reader and the tag coils at this zone but also because of the presence of the resonator).

In the conventional system, the magnitude of the input impedance has two maxima of 2.2 Ω corresponding to the edges of the reader coil and a minimum value of 0.5 Ω at the surface of the reader coil. The phase of the input impedance is also changed by the added resonator. In this case, the evolution of the phase of the equivalent input impedance has two parts: positive and negative values, between the two parts, we can see a zero near to the centre of the reader coil ($y = 0$ mm). From the results, both the magnitude and the phase of the input impedance in parallel and perpendicular configuration are changed. This variation is due to the added resonator because of the variation of the impedance matrix parameters. Also, we can note that the input impedance is also varying according to the tag positioning; this variation is negligible in the parallel configuration compared with the effect of the added resonator. The influence of the tag misalignment on the input impedance is more important in the case of the perpendicular configuration

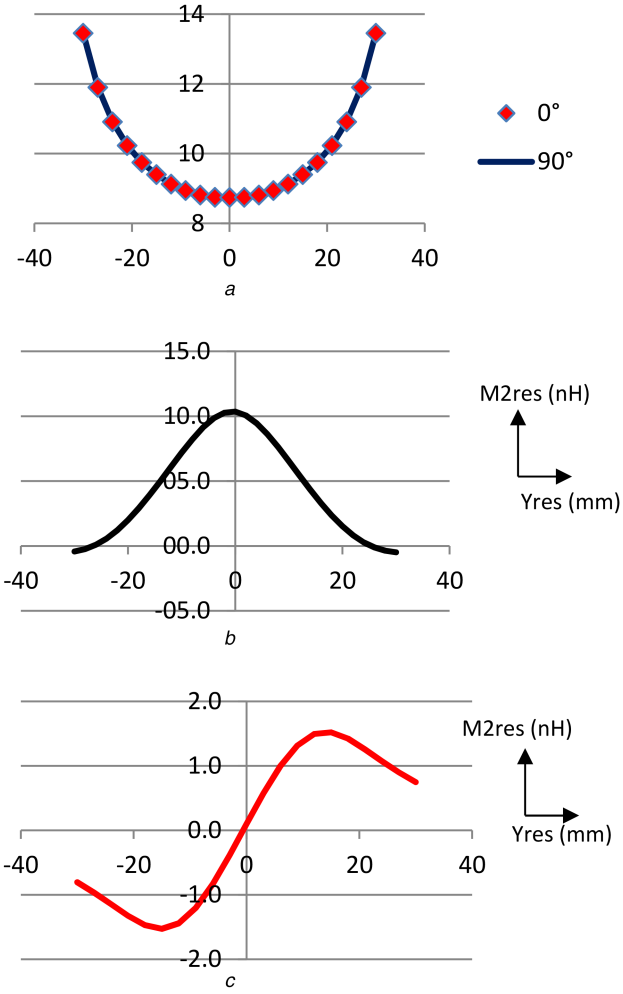

Fig. 3 *The mutual inductances (M_{1res}) and (M_{2res}) for different resonator positioning (−30 mm < Y_{res} < 30 mm)*

(a) ($M_{1\text{res}}$) between the reader coil and the resonator, ***(b)*** ($M_{2\text{res}}$) between the tag coil and the resonator in parallel configuration and ***(c)*** ($M_{2\text{res}}$) between the tag coil and the resonator in perpendicular configuration for different resonator positioning (−30 mm < Y_{res} < 30 mm)

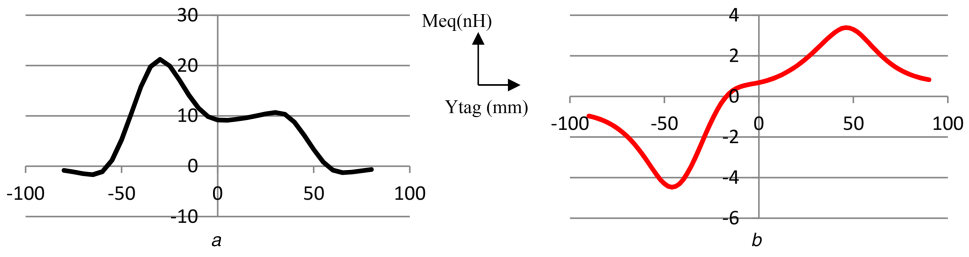

Fig. 4 *Equivalent mutual inductance (M_{eq}) between the reader coil including one resonator (positioned at $Y_{res} = -30$ mm) and the tag coil, respectively, in* ***(a)*** Parallel configuration, ***(b)*** Perpendicular configuration for tag misalignment: from ($Y_{\text{tag}} = -100$ mm) to ($Y_{\text{tag}} = 100$ mm)

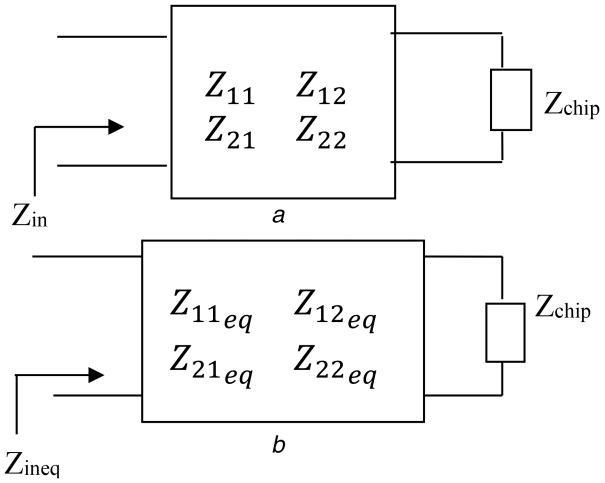

Fig. 5 *Equivalent electrical circuit of RFID system*
(a) Without resonator, ***(b)*** With resonator

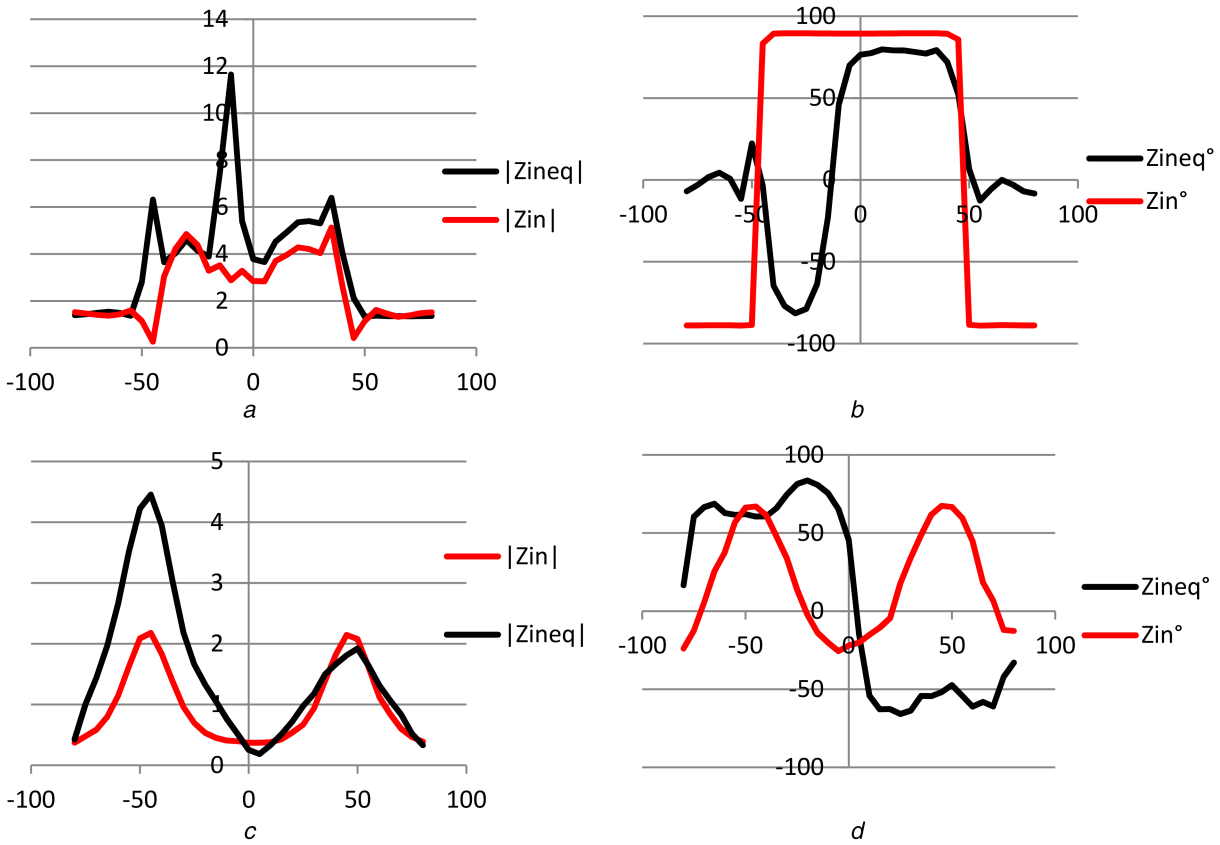

Fig. 6 *Magnitude and phase of input impedance and equivalent input impedance*
(a) Magnitude of input impedance ($|Z_{in}|$) and equivalent input impedance ($|Z_{ineq}|$) in parallel configuration, ***(b)*** and in perpendicular configuration, ***(c)*** Phase of input impedance ((Zin)°) and equivalent input impedance ((Zineq)°) in parallel configuration and ***(d)*** in perpendicular configuration

4 Measures

A reader antenna of rectangular shape (10×61 cm^2) is fabricated. The design is produced using a copper film glued on a transparent sheet. The reader antenna has one coil turn. The tag has a circular shape with a radius of 1.2 cm. The resonators have a rectangular shape of 8×5.7 cm^2 (Fig. 7). The tag coil and resonators correspond, respectively, to 0.74 and 7.37% of the reader surface. The added resonator reduced the size ratio between the tag and the reader coil: the tag coil corresponds to 10% of the resonator surface.

In measures part, a reader structure including two resonators is studied. The problem of frequency shift according to the number of resonators on the surface of the reader is studied. The second part of measure concerns RFID detection.

4.1 Frequency shift in RFID system

The equivalent electrical model corresponding to the proposed reader coil including two resonators is shown in Fig. 7*c*. The reader and tag coil are presented by two inductances in serial with capacitances (to find the resonance frequency). The resonators correspond to two RLC circuits. In this first part of measures, the shift frequency in the reader coil is evaluated according to the number of resonators. As is proved in the calculation part and simulation results, the added resonator modifies all the impedance matrix parameters. A shift in the phase of the input impedance is then seen in both parallel and perpendicular configurations. Two resonators are used in the experimental studies. Using the equivalent electrical model of the system (Fig. 7*c*), the equivalent impedance matrix parameters are calculated in this part. As seen in the electrical model, mutual coupling is generated between the

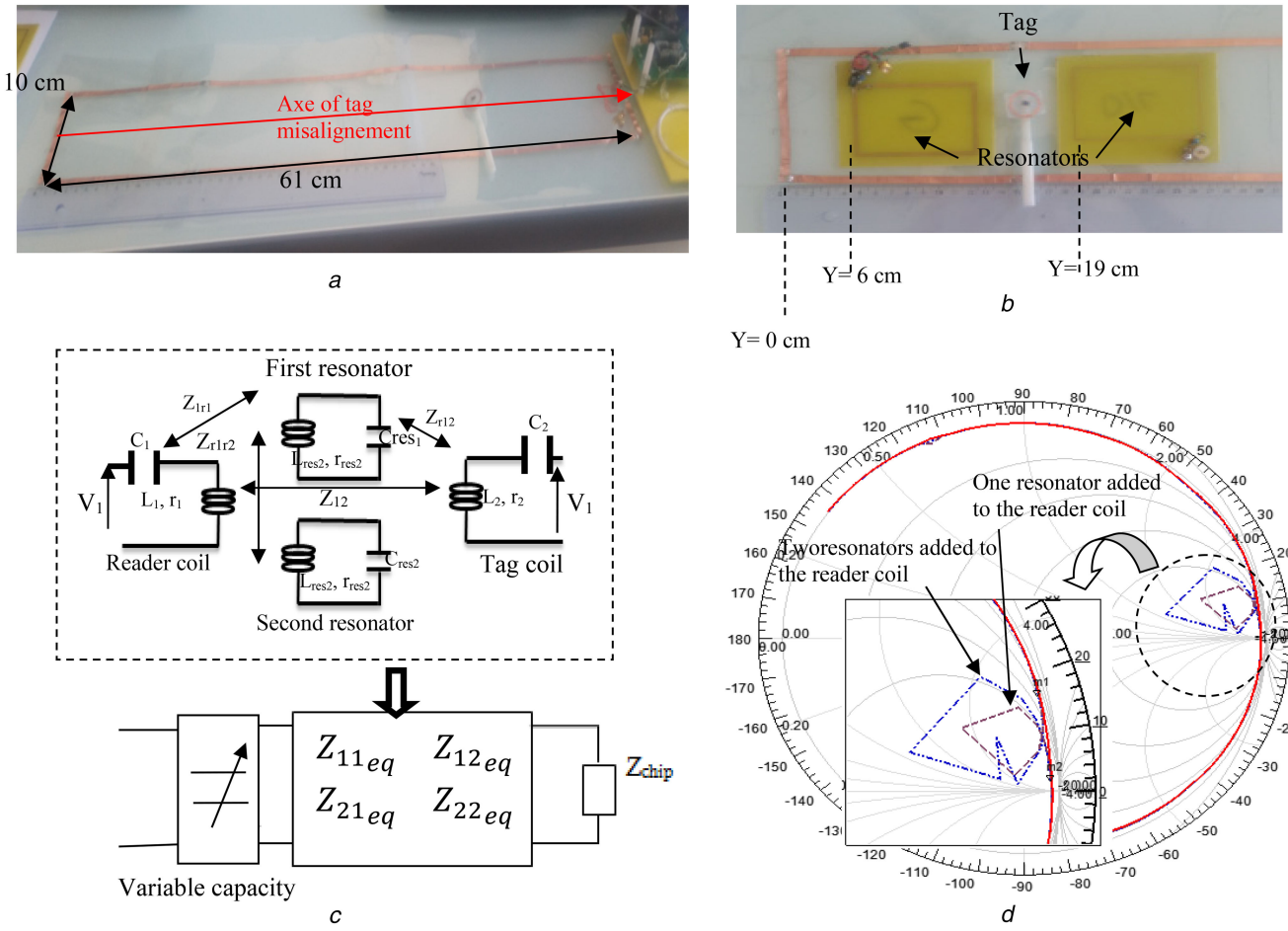

Fig. 7 *Fabricated RFID prototype*

(a) Without a resonator, ***(b)*** With two resonators, ***(c)*** Its equivalent electrical model, ***(d)*** Measures of impedance matrix parameters without resonator with one resonator and with two resonators

resonators and the reader coil, the resonators and the tag coil, and between the two resonators. To evaluate the influence of the added resonators, the equivalent impedance parameters are calculated by using the following equation:

$$
\begin{aligned}
Z_{11_{eq}} &= \left(Z_{11} + \frac{Z_{1r1}^2}{Z_{cr1} - Z_{r1}}\right) + \frac{\left(Z_{1r2} + \frac{Z_{2r1}Z_{r1r2}}{Z_{cr1} - Z_{r1}}\right)^2}{Z_{cr2} - \left(Z_{r2} + \frac{Z_{r1r2}^2}{Z_{cr1} - Z_{r1}}\right)}, \\
Z_{12_{eq}} &= \left(Z_{12} + \frac{Z_{1r1}Z_{r1}^2}{Z_{cr1} - Z_{r1}}\right) \\
&\quad + \frac{\left(Z_{1r2} + \frac{Z_{1r2}Z_{r2r1}}{Z_{cr1} - Z_{r1}}\right)\left(Z_{r2}^2 + \frac{Z_{r2r1}Z_{r1r2}}{Z_{cr1} - Z_{r1}}\right)}{Z_{cr2} - \left(Z_{r2} + \frac{Z_{r1r2}^2}{Z_{cr1} - Z_{r1}}\right)}, \\
Z_{21_{eq}} &= \left(Z_{21} + \frac{Z_{r1}^2 Z_{1r1}}{Z_{cr1} - Z_{r1}}\right) \\
&\quad + \frac{\left(Z_{2r1} + \frac{Z_{r1r2}Z_{r2r2}}{Z_{cr1} - Z_{r1}}\right)\left(Z_{r11} + \frac{Z_{r1r2}Z_{r21}}{Z_{cr1} - Z_{r1}}\right)}{Z_{cr2} - \left(Z_{r2} + \frac{Z_{r1r2}^2}{Z_{cr1} - Z_{r1}}\right)}, \\
Z_{22_{eq}} &= \left(Z_{22} + \frac{Z_{2r1}^2}{Z_{cr1} - Z_{r1}}\right) + \frac{\left(Z_{2r2} + \frac{Z_{2r1}Z_{r1r2}}{Z_{cr1} - Z_{r1}}\right)^2}{Z_{cr2} - \left(Z_{r2} + \frac{Z_{r1r2}^2}{Z_{cr1} - Z_{r1}}\right)},
\end{aligned}
\tag{6}
$$

where Z_{11}, Z_{22} are the impedances of the reader and the tag coil; Z_{1r1} (or Z_{r11}), Z_{1r2} (or Z_{1r2}) are, respectively, the mutual impedances between the reader coil and the first resonator, reader coil, and the second resonator; Z_{r1r2} (or Z_{r1r2}) is the mutual impedances between the first and second resonator; Z_{cr1}, Z_{cr2}, Z_{r1}, and Z_{r2} are, respectively, the imaginary and real parts of the impedances of the resonators.

From (6), the equivalent impedance parameters are changed compared with (1) and (2). New parameters appear like: the electrical properties of the second resonator, mutual impedance between the second resonator and the reader coil, the mutual impedance between the second resonator and the tag coil and also the mutual impedance between the second resonator and the first resonator.

The first part of measurements concerns, the frequency shift in the reader coil due to the added resonators. The measures are done at the resonance frequency of the reader coil (15.18 MHz) using a vector network analyser. The shift of resonance frequency (Δf) is reported in Table 2.

The added first resonator creates a frequency shift of 0.19 MHz, the reader coil, the second added resonator improve this shift to 0.38 MHz. The maximum effect of the resonators on the reader coil is seen between 12.6 and 14.9 MHz around the resonance frequency of the resonators (Fig. 7*d*). From the results, we can note the necessity of the correction of the shift frequency because of the added resonators. In our case, a variable capacity is added to the reader coil. It is used to find the resonance frequency at 13.56 MHz after added all the resonators. Our method corresponds to the electrical model in Fig. 7*c*. Also, an optimisation of the resonators positioning on the reader coil is done. Optimisation is principally done to limit the frequency shift due to the magnetic coupling between resonators. From this study, the resonators are positioned, respectively, at 6 and 19 cm from the edges of the reader coil. The distance between them is fixed at 5 cm (Fig. 7*b*).

Table 2 Frequency shift in RFID system

Prototype	With one resonator, MHz	With two resonators, MHz
Δf, MHz	0.197	0.384
f_2, MHz	15.38	15.57

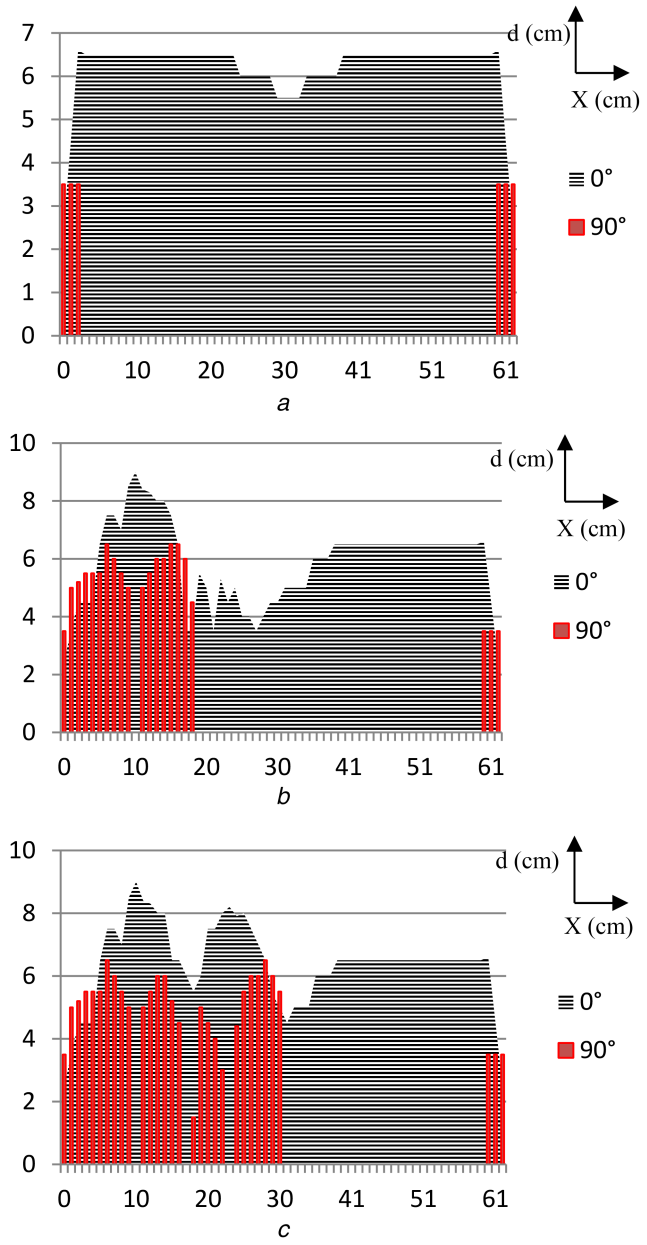

Fig. 8 *RFID detection using prototype*
(a) Without resonator, ***(b)*** With one resonator, ***(c)*** With two resonators. The tag misalignment id above the reader surface at $X = 0$ cm from $Y = 0$ cm to 61 cm (as seen in Fig. 7*a*)

4.2 RFID detection

The proposed approach is validated by measurements of RFID detection. An experimental test of increasing detection volume (a distance of detection) and surface (at different positions on the surface of the reader coil) by adding resonators on the reader coil was made using an RFID reader from Ib Technologies. The prototypes in Fig. 7*a* and *b* are used in our tests. The measures are reported in Fig. 8 for parallel and perpendicular configuration. The tag misalignment corresponds to its displacement on the reader surface. (X, Y) axis in Fig. 8, correspond, respectively, to the misalignment of the tag according to the length of the reader coil, and the distance of the RFID detection. The tag misalignment corresponds to the middle of the reader coil according to its width (see Fig. 7*a*). The result of tag detection in parallel and perpendicular configurations without resonators (a), with one resonator (b) and with two resonators (c) are reported in (Fig. 8).

For a reader coil without a resonator, the tag is detected all over the surface of the reader coil in a parallel configuration. In this case, the distance of detection has a maximum value of 6.5 cm from the edges of the reader coil to its centre and the minimum value at the centre of the reader coil (5.5 cm). For perpendicular configuration, the tag is only detected at the edges of the reader coil for a distance of 3.5 cm. These results confirm the simulated results.

For a prototype including one resonator, both the volume and the surface of detection for parallel and perpendicular configuration are increased. In the parallel configuration, the distance of detection is improved at the surface of the resonator (from 6.5 to 9 cm). The minimum value of the distance of detection is shifted by 2 cm (from 5.5 to 3.5 cm). For the perpendicular configuration, the surface of detection is improved; the tag is detection from the edges of the reader coil (0 mm) to 19 cm. Zero detection is seen at the centre of the resonator 10 cm and at the surface of the reader coil which does not contain the resonator (from 20 to 61 cm).

For a prototype with two resonators, in the parallel configuration, three maxima of detection are seen at the surface of the reader coil: 9, 8 and 6.5 cm corresponding, respectively, to the surface of the first resonator, the second resonator and the surface of the reader coil which does not include resonators. In the perpendicular configuration, the distance of detection has a maximum of 6.5 cm at the edges of the resonators and presents four zeros corresponding to the centres of the two resonators, the surface between them and the surface of the reader coil which does not include resonators. At the edge of the reader coil (61 cm), the distance of detection corresponds to the case without the resonator.

From the results, the proposed concept of added resonators is confirmed. The volume and surface of detection are improved in both parallel and perpendicular configurations. More resonators can be added to the surface of the reader coil (from 30 to 61 cm) to ensure the continuity of detection.

5 Conclusion

A reader coil including resonators is proposed in this study. Firstly, a prototype including one resonator is studied by calculation and simulation to demonstrate the interest of added resonators in the case of RFID application. From the results, optimising communication between the reader and the tag coils depends on the resonators positioning and their electrical properties. The added resonators create a frequency shift in the input impedance of the reader coil, the frequency shift is studied by the simulation of the input impedance in the case of prototypes with and without the resonator and confirmed by measures. Finally, measures of RFID detection are reported to confirm the improvement of both surface and volume of detection in the case of the misaligned tag in parallel and perpendicular configurations.

6 References

[1] Berger, A., Agostinelli, M., Vesti, S., *et al.*: 'A wireless charging system applying phase-shift and amplitude control to maximize efficiency and extractable power', *IEEE Trans. Power Electron.*, 2015, **30**, pp. 6336–6348

[2] Kim, S., Ho, J.S., Poon, A.S.: 'Wireless power transfer to miniature implants: transmitter optimization', *IEEE Trans. Antennas Propag.*, 2012, **60**, pp. 4838–4845

[3] Ho, J.S., Kim, S., Poon, A.S.: 'Midfield wireless powering for implantable systems', *Proc. IEEE*, 2015, **101**, pp. 1369–1378

[4] Jow, U.M., McMenamin, P., Kiani, M., *et al.*: 'Enercage: a smart experimental arena with scalable architecture for behavioral experiments', *IEEE Trans. Biomed. Eng.*, 2014, **61**, pp. 139–148

[5] Wang, C.S., Stielau, O.H., Covic, G.A.: 'Design considerations for a contactless electric vehicle battery charger', *IEEE Trans. Ind. Electron.*, 2005, **52**, pp. 1308–1314

[6] Jang, Y., Jovanovic, M.M.: 'A contactless electrical energy transmission system for portable-telephone battery chargers', *IEEE Ind. Electron.*, 2003, **50**, pp. 520–527

[7] Babic, S.I., Sirois, F., Akyel, C.: 'Validity check of mutual inductance formulas for circular filaments with lateral and angular misalignments', *Prog. Electromagn. Res.*, 2009, **8**, pp. 15–26

[8] Zierhofer, C., Hochmair, E.: 'Geometric approach for coupling enhancement of magnetically coupled coils', *IEEE Trans. Biomed. Eng.*, 1996, **43**, pp. 708–714

[9] Wang, B., Yerazunis, W., Teo, K.H.: 'Wireless power transfer: metamaterials and array of coupled resonators', *Proc. IEEE*, 2013, **101**, pp. 1359–1368

[10] Berger, A., Agostinelli, M., Vesti, S., *et al.*: 'A planar magnetically coupled resonant wireless power transfer system using printed spiral coils', *IEEE Antennas Wirel. Propag. Lett.*, 2014, **13**, pp. 1648–1651

[11] Diet, A., Grzeskowiak, M., Le Bihan, Y., *et al.*: 'Improving LF reader antenna volume of detection, for RFID token tag, with a combination of ICLs and in/out-of phase multiple-loops structures'. IEEE RFID Technology and Applications Conf. (RFID-TA), 2014, pp. 208–213

[12] Hwang, H., Moon, J., Lee, B., *et al.*: 'An analysis of magnetic resonance coupling effects on wireless power transfer by coil inductance and placement', *IEEE Trans. Consum. Electron.*, 2014, **60**, pp. 203–209

[13] Fotopoulou, K., Flynn, B.W.: 'Wireless power transfer in loosely coupled links: coil misalignment model', *IEEE Trans. Magn.*, 2011, **47**, pp. 416–430

[14] Eteng, A.A., Rahim, S.K.A., Leow, C.Y., *et al.*: 'Loop antenna design for lateral H-field uniformity in misaligned HF-RFID links'. IEEE Symp. on Wireless Technology & Applications (ISWTA), 2014, pp. 92–95

[15] Grzeskowiak, M., Diet, A., Diao, P.S., *et al.*: 'Pebbles tracking thanks to RFID LF multi-loops inductively coupled reader', *Prog. Electromagn. Res. C*, 2014, **55**, pp. 129–137

[16] D'hoe, K., Goemaere, J., Stevens, N., *et al.*: 'Automated design of an HF RFID loop antenna based on parametric geometry modification'. IEEE Int. Conf. on RFID, 2014, pp. 1–7

[17] Benamara, M., Grzeskowiak, M., Diet, A., *et al.*: 'Calculation of the equivalent mutual impedance in complex HF RFID systems'. IEEE Int. Conf. on Applied Electromagnetics and Communications (ICECOM), Dubrovnik, 2016

[18] Finkenzeller, K.: '*RFID handbook : Fundamentals and applications in contactless smart cards and identification*' (Wiley, New York, 2003, 3rd edn.)

[19] Hackl, S., Lanschützer, C., Raggam, P., *et al.*: 'A novel method for determining the mutual inductance for 13.56 MHz RFID systems', *Commun. Syst. Netw. Digit. Signal Process.*, 2008, pp. 297–300

[20] Benamara, M., Grzeskowiak, M., Diet, A., *et al.*: 'Reader antenna including resonators for HF RFID detection'. 2016 Loughborough Antennas & Propagation Conf. (LAPC), 2016